# Supplementary Information for "Tuning the oxygen vacancy formation energy of ceria by doping first row transition metals for aerobic oxidation desulfurization"

**Xiaoshuang Tian,[a] Shenhao Huang,[b] Yuhan Tang,[a] Haiyang Feng,[a] Lizhao Liu,*[c] Hong Liu,[a] and Jiasheng Wang*[a]**

[a.] *State Key Laboratory of Fine Chemicals, School of Chemical Engineering, Ocean and Life Sciences, Dalian University of Technology, Panjin, 124221, China.*

[b.] *Leicester International Institute, Dalian University of Technology, Panjin, 124221, China.*

[c.] *School of General Education, Dalian University of Technology, Panjin, 124221, China.*

*E-mail: lizhao_liu@dlut.edu.cn; jswang@dlut.edu.cn*

## 1 Experimental

### 1.1 Materials

Cerium nitrate hexahydrate ($Ce(NO_3)_3·6H_2O$), scandium nitrate hydrate ($Sc(NO_3)_3·xH_2O$), tetraethyl titanate ($Ti(OC_4H_9)_4$), Chromium nitrate nonahydrate ($Cr(NO_3)_3·9H_2O$), Manganese nitrate ($Mn(NO_3)_3·4H_2O$), Iron nitrate nonahydrate ($Fe(NO_3)_3·9H_2O$), cobalt nitrate hexahydrate ($Co(NO_3)_3·6H_2O$), nickel nitrate ($Ni(NO_3)_2·6H_2O$), copper nitrate trihydrate ($Cu(NO_3)_2·3H_2O$), zinc nitrate ($Zn(NO_3)_2·6H_2O$), sodium hydroxide (NaOH), ammonium metavanadate ($NH_4VO_3$), dibenzothiophene ($C_{12}H_8S$), decahydronaphthalene ($C_{10}H_{18}$), dimethyl sulfoxide (DMSO), p-benzoquinone (BQ) were all analytical grade and purchased from Shanghai Aladdin Biochemical Technology Co., Ltd. These reagents required no further processing and could be used directly. Ultrapure water was used throughout the entire experiment.

### 1.2 Synthesis of $CeMO_x$ support

3.6 g of $Ce(NO_3)_3·6H_2O$ and 0.37 g of $Cr(NO_3)_3·9H_2O$ were dissolved in 10 mL ultrapure water. Next, 70 mL of 7 M NaOH solution was added to the above solution while maintaining stirring for 30 min. Subsequently, the resulting slurry was transferred to a 100 mL Teflon-lined autoclave reactor and maintained at 100°C in an oven for 24 h. After natural cooling to room temperature, the precipitate was collected and washed several times with ultrapure water until the solution pH reached 7. The obtained product was dried in an electric oven at 100°C for 12 h and ground in a mortar and pestle to yield a fine powder. Finally, the powder was calcined in a static air atmosphere at 500°C (with a heating rate of 3°C/min) for 5 h in a calcination furnace to obtain the $CeCrO_X$ support. Other metal-doped $CeMO_X$ were prepared using the same procedure with corresponding precursors.

### 1.3 Synthesis of $VO_x/CeMO_x$

1.0 g of $CeMO_X$ and 0.078 g of $NH_4VO_3$ were dissolved in 10 mL of ultrapure water and stirred continuously at 60°C for 2 h. The resulting slurry was dried in an electric oven at 100°C for 12 h and ground into a fine powder. Finally, the powder was calcined in a calcination furnace at 600°C (with a heating rate of 3°C/min) for 5 h under static air to obtain $VO_X/CeMO_X$.

### 1.4 Characterization

The apparent morphological structure of the catalyst was observed using an scanning electron microscope (Nova Nano SEM 450, FEI, USA) and energy-dispersive X-ray spectroscopy (EDS). Crystal phases were analyzed by X-ray diffraction (XRD, Lab XRD—7000s) equipped with Cu Kα radiation at the voltage of 120 kV and a current of 100 mA, recorded with 2θ varying from 10 to 90° with a scanning speed of 5°/min. Laser Confocal Micro-Raman Spectrometer (inVia, Renishaw, UK) were measured using a laser micro-Raman spectrometer in the 200-800 $cm^{-1}$ range with a spectral resolution of 1 $cm^{-1}$. The excitation source was an $Ar^+$ ion laser ($\lambda$ = 514 nm) with a laser power of 20 mW. The chemical composition and functional groups of sorbents were investigated with the help of FTIR spectrometer (PerkinElmer, USA) carried out by a Spectrum 3 system. X-ray photoelectron spectroscopy (XPS) was performed on a VG ESCALAB MKII X-ray photoelectron spectrometer (ESCALAB250Xi, Thermo Fisher Scientific, UK) equipped with a monochromatic Al Kα X-ray source. Electron paramagnetic resonance (EPR) was performed using a Bruker model A200–9.5/12 paramagnetic resonance spectrometer.

### 1.5 Oxidative desulfurization experiments

0.045 g of DBT was dissolved in 100 mL of decahydronaphthalene to prepare a 500 ppm simulated oil. The reaction was conducted in a 50 mL double-neck flask. 20 mL of simulated oil

and 100 mg of catalyst were added to the flask. The mixture was heated and stirred at 80°C under continuous oxygen flow (150 mL/min). Samples of 0.5 mL were taken at reaction times of 0 h, 2 h, 4 h, 6 h, and 10 h. After 10 h, the oxygen flow was stopped, and the mixture was cooled to room temperature. Extracted samples were filtered through membrane filters to remove catalyst. DBT content in pre-reaction, reaction, and post-reaction samples was analyzed by gas chromatography (GC). Conversion rates at each time point were calculated using the internal standard method.

The gas chromatograph (GC) analysis was performed using an Agilent 7820A instrument (Agilent Technologies Inc., USA) equipped with a flame ionization detector (FID) and a capillary column (30 m length, 320 μm inner diameter, 0.25 μm film thickness). The temperature program for separation was initiated at 110°C and held for 1 min, followed by a gradual increase to 250°C at a rate of 10°C/min. Both the injector and detector temperatures were maintained at 300°C throughout the analysis.

To establish the calibration curve for dibenzothiophene (DBT) quantification, simulated oil standard solutions with varying DBT concentrations were prepared by dissolving precise masses of DBT in decahydronaphthalene (Fig. S1). A fixed amount of n-tetradecane was added to each solution as an internal standard to normalize analytical variability. Gas chromatography (GC) analysis was performed under the specified conditions (Agilent 7820A, FID detector), and the peak area ratios of DBT to n-tetradecane were recorded for each concentration. A linear regression model was constructed by plotting the DBT/internal standard peak area ratio against the corresponding DBT concentration.

$$\eta(\%) = \frac{C_0 - C_t}{C_0} \times 100\%.$$

$C_0$: initial sulfur content, mol $L^{-1}$ ;

$C_t$: Sulfur Content at Different Reaction Times, mol $L^{-1}$.

### 1.6 Catalyst cycling stability test

The catalyst was subjected to reaction under the following conditions: a reaction temperature of 80°C, an oxygen flow rate of 150 mL/min, and a reaction time of 10 hours. After each oxygen-oxidative desulfurization reaction, the catalyst was washed with acetone, centrifuged to dry, and then subjected to the next cycle of testing. The catalyst underwent a total of five reaction cycles.

### 1.7 Heat filtration test

Before the reaction, preheat the glass rod, beaker, and short-neck funnel as needed. Prepare filter paper and moisten it with a small amount of hot solvent to ensure it fits snugly inside the funnel. Slowly pour the simulated oil, which has reacted for 4 hours, into the funnel using the glass rod. Conduct the entire filtration process in an oven at 100°C. Subject the filtered simulated oil to an oxygen oxidation desulfurization test, and draw samples of the reaction mixture every hour for gas-phase analysis.

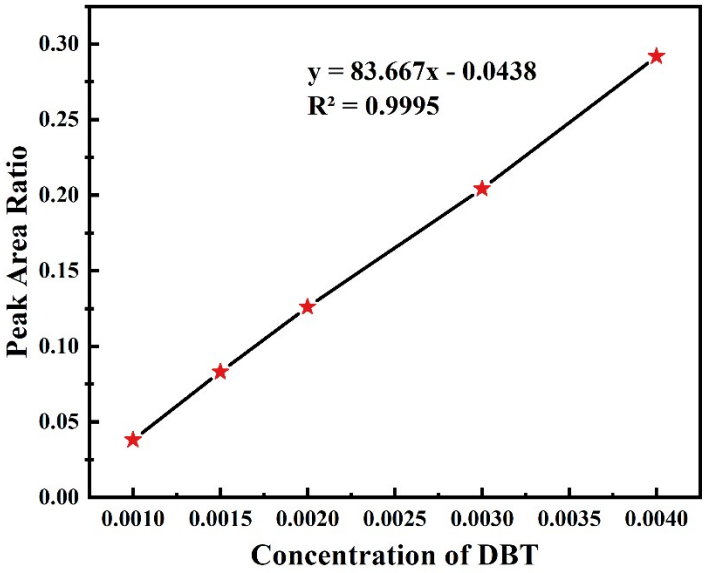


Fig. S1 DBT Calibration Curve.

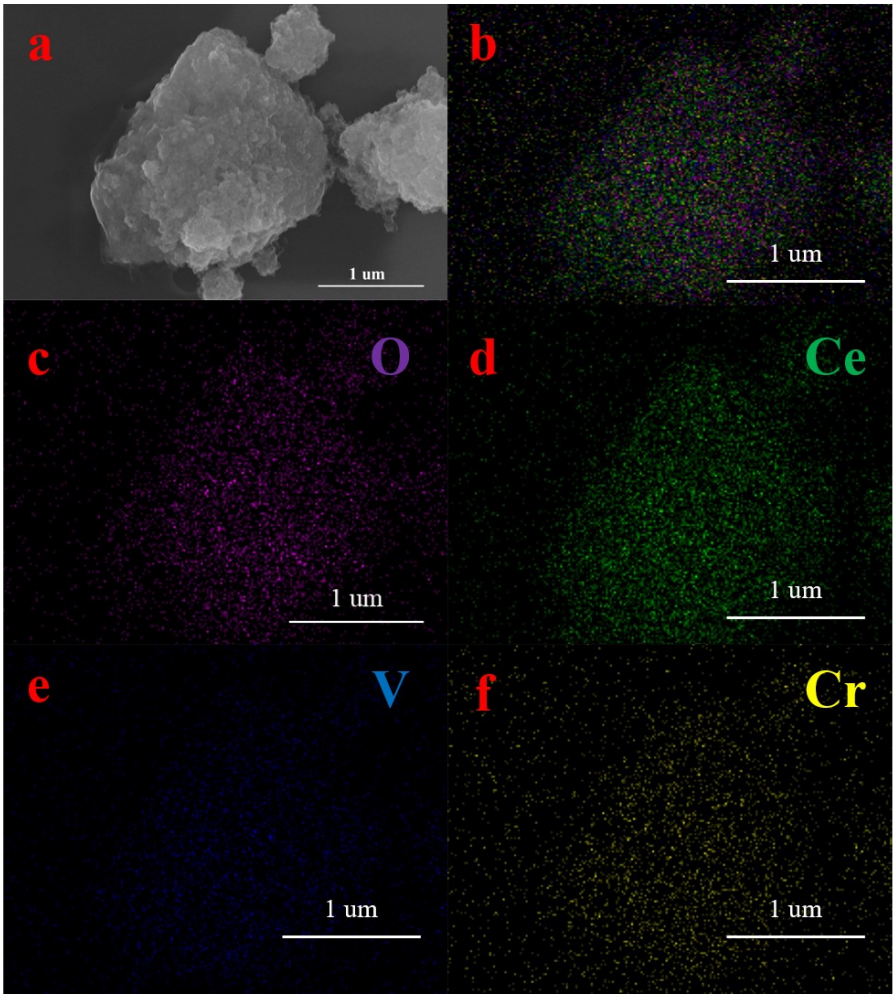


Fig. S2 SEM/EDS analysis of $VO_x/CeCrO_x$ catalysts: (a) SEM; (b) Overlaid elements; (c) O; (d) Ce; (e) V; (f) Cr.

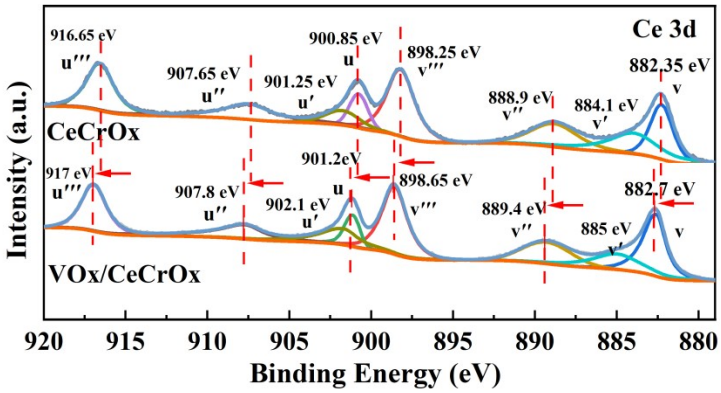


Fig. S3 XPS spectra of Ce 3d before and after loading metal on the catalyst.

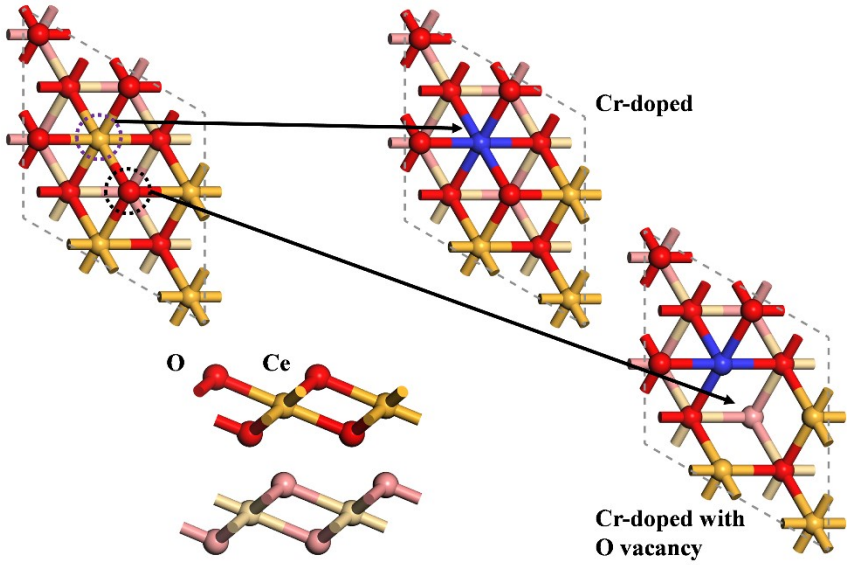


Fig. S4 Schematics of M-doped $CeO_2$ (M = Sc, Ti, V, Cr, Mn, Fe, Co, Ni, Cu and Zn) and the counterpart with an oxygen vacancy.

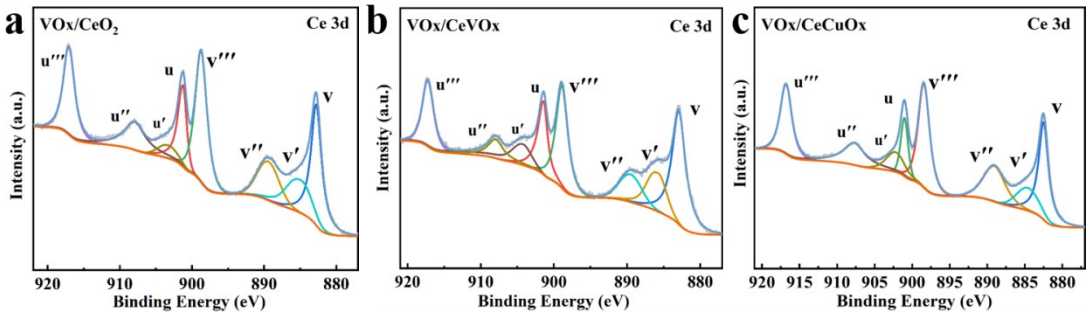


Fig. S5 XPS analysis of Ce 3d for $VO_x/CeO_2$ and $VO_x/CeMO_x$ (M = V, Cu) catalysts

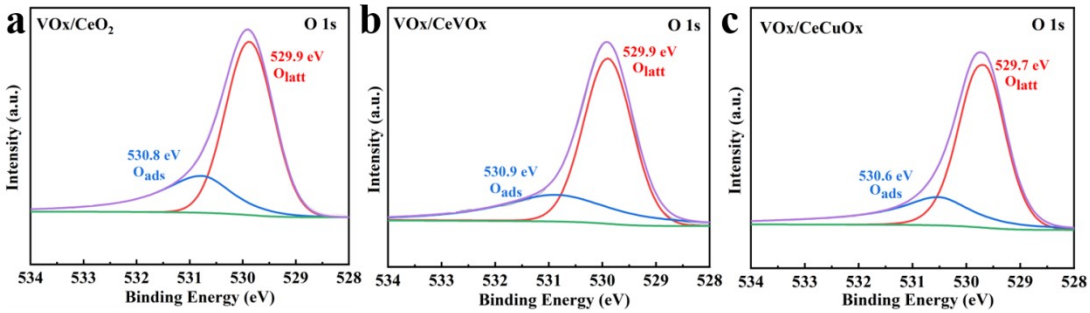


Fig. S6 XPS analysis of O 1s for $VO_x/CeO_2$ and $VO_x/CeMO_x$ (M = V, Cu) catalysts.

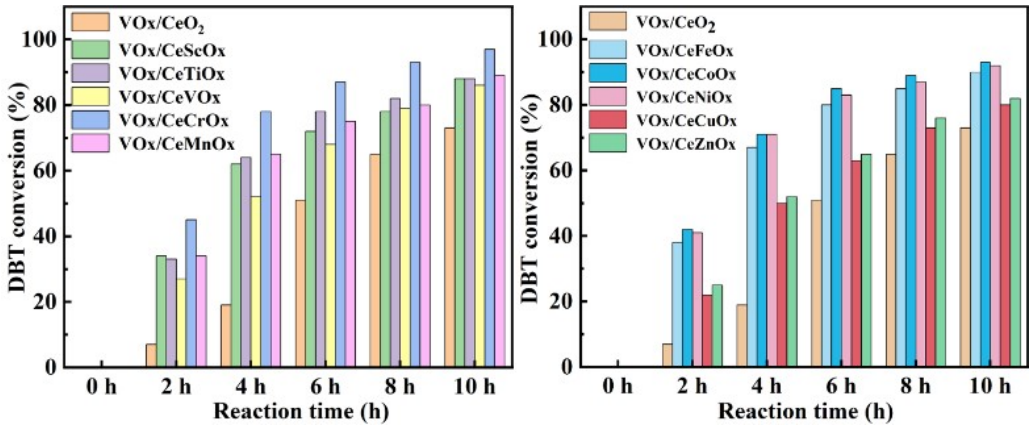


Fig. S7 The catalytic activity of the prepared $VO_x/CeMO_x$ catalysts at 80 °C.

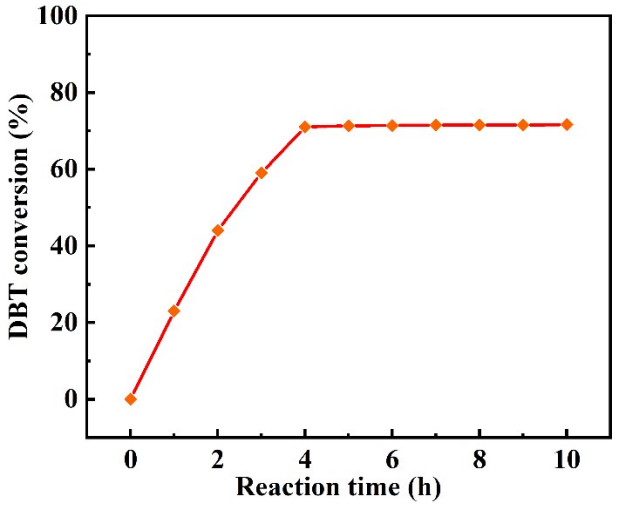


Fig. S8 Thermal filtration test of $VO_x/CeMO_x$ catalyst after 5 cycles.

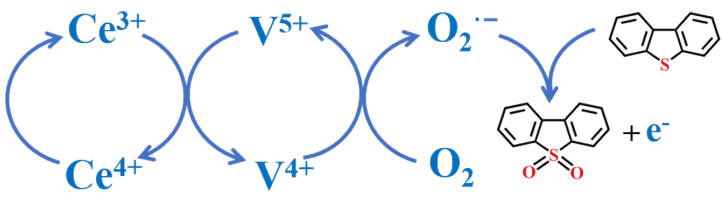


Fig. S9 The proposed catalytic mechanism of AODS on $VO_x/CeCrO_x$ catalyst.

Table S1 Calculated oxygen vacancy formation energy for $VO_x/CeMO_x$ catalysts.

| Catalysts | $E_{vac}$/eV |
|---|---|
| $CeO_2$-Ov-tp | -0.183 |
| $CeO_2$-Cr-Ov-top | 0.833 |
| $CeO_2$-Co-Ov-top | -0.802 |
| $CeO_2$-Ni-Ov-top | -0.787 |
| $CeO_2$-Fe-Ov-top | -0.775 |
| $CeO_2$-Mn-Ov-top | -0.716 |
| $CeO_2$-Ti-Ov-top | -0.632 |
| $CeO_2$-Sc-Ov-top | -0.618 |
| $CeO_2$-V-Ov-top | -0.612 |
| $CeO_2$-Zn-Ov-top | -0.415 |
| $CeO_2$-Cu-Ov-top | -0.308 |

Table S2 Proportion of $Ce^{3+}$ and $Ce^{4+}$ in $VOx/CeO_2$ and VOx/CeMOx (M = V, Cr, Cu) catalysts.

| **catalyst** | **v′/u′** | **v/u、v″/u″、v″/u′** | **$Ce^{3+}$:$Ce^{4+}$** |
|---|---|---|---|
| $VOx/CeO_2$ | 0.139 | 0.285 | 0.160 |
| VOx/CeVOx | 0.175 | 0.825 | 0.210 |
| VOx/CeCrOx | 0.189 | 0.811 | 0.233 |
| VOx/CeCuOx | 0.140 | 0.860 | 0.163 |

Table S3 Proportion of different oxygen species in $VO_x/CeO_2$ and $VO_x/CeMO_x$ (M = V, Cr, Cu) catalysts.

| catalyst | Olatt | Oads | Oads: Olatt |
|---|---|---|---|
| VOx/$CeO_2$ | 0.715 | 0.285 | 0.40 |
| VOx/CeVOx | 0.700 | 0.300 | 0.43 |
| VOx/CeCrOx | 0.680 | 0.320 | 0.47 |
| VOx/CeCuOx | 0.705 | 0.295 | 0.42 |

Table S4 The activity comparison of $VO_x/CeMO_x$ with the reported metal oxide catalysts.

| Catalyst | Reaction temperature (°C) | Conversion (%) | Ref |
|---|---|---|---|
| $VO_x$/ $CeCrO_x$ | 80 | 100 | This work |
| $[C_4VIM]PMoV_2$ | 120 | 100 | 1 |
| Co-Fe-Mo | 120 | 100 | 2 |
| V-BNO | 125 | 100 | 3 |
| $V_2O_5$/BNNS | 125 | 99.6 | 4 |
| CoMo nanosheet | 100 | 100 | 5 |
| Co-Mo-O | 100 | 83 | 6 |
| MoOx/MC-600 | 120 | 100 | 7 |
| CeW/AC | 150 | 99.9 | 8 |


1. M. Zhang, J. Liu, H. Li, Y. Wei, Y. Fu, W. Liao, L. Zhu, G. Chen, W. Zhu and H. Li, *Appl. Catal. B: Environ.*, 2020, **271**, 118936.
2. Y. Song, J. Bai, S. Jiang, H. Yang, L. Yang, D. Wei, L. Bai, W. Wang, Y. Liang and H. Chen, *Fuel*, 2021, **306**, 121751.
3. L. Dai, Y. Wei, X. Xu, P. Wu, M. Zhang, C. Wang, H. Li, Q. Zhang, H. Li and W. Zhu, *ChemCatChem*, 2020, **12**, 1734–1742.
4. C. Wang, Y. Qiu, H. Wu, W. Yang, Q. Zhu, Z. Chen, S. Xun, W. Zhu and H. Li, *Fuel*, 2020, **270**, 117498.
5. Y. Dong, J. Zhang, Z. Ma, H. Xu, H. Yang, L. Yang, L. Bai, D. Wei, W. Wang and H. Chen, *Chem. Commun.*, 2019, **55**, 13995–13998.
6. Q. Zhang, J. Zhang, H. Yang, D. Wei, W. Wang, Y. Dong, Y. Liu, L. Yang, L. Bai and H. Chen, *Catal. Sci. Technol.*, 2019, **9**, 2915–2922.
7. W. Jiang, J. Xiao, L. Dong, C. Wang, H. Li, Y. Luo, W. Zhu and H. Li, *ACS Sustain. Chem. Eng.*, 2019, **7**, 15755–15761.
8. M. Abdulhassan, H. H. Alwan, *Results Eng.*, 2024, **23**, 102557.